RESEARCH ARTICLE

Trans-resveratrol simultaneously increases cytoplasmic Ca^{2+} levels and nitric oxide release in human endothelial cells

Jacobo Elíes, Andrea Cuíñas, Verónica García-Morales, Francisco Orallo**, and Manuel Campos-Toimil*

Departamento de Farmacoloxía, Universidade de Santiago de Compostela, Santiago de Compostela, Spain

Received: April 6, 2011
Revised: May 12, 2011
Accepted: May 16, 2011

Scope: The aim of this study was to investigate whether the dietary polyphenol *trans*-resveratrol (*t*-Resv) increases $[Ca^{2+}]_c$ in endothelial cells, leading to a simultaneous augmentation of nitric oxide (NO) biosynthesis.

Methods and results: We have separately and simultaneously measured $[Ca^{2+}]_c$ and NO in human endothelial cells using the Ca^{2+} indicator fura-2 and the NO-sensitive fluorescent probe 4,5-diaminofluorescein. In ~30% of cells, *t*-Resv (30 μM) induced an increase in $[Ca^{2+}]_c$ with a transient as well as sustained component and a simultaneous increase in NO biosynthesis. This effect was reduced by non-selective Ca^{2+} channel blockers, inhibition of intracellular Ca^{2+} release, inhibition of endothelial nitric oxide synthase (eNOS) and, to a lesser extent, inhibition of extracellular signal-regulated kinase 1/2 (ERK 1/2) or 5′ adenosine monophosphate-activated protein kinase (AMPK). *t*-Resv did not modify in vitro eNOS activity, suggesting that the observed stimulation of NO generation proceeds via mobilisation of Ca^{2+} and not through direct effects on eNOS.

Conclusion: We therefore show, for the first time, that *t*-Resv induces a concentration-dependent, simultaneous increase in $[Ca^{2+}]_c$ and NO biosynthesis that could be linked to its endothelium-dependent vasorelaxant effect. Under the assumption that *t*-Resv exhibits similar behaviour in human blood vessels in vivo, the pharmacological properties described here may contribute to the beneficial cardiovascular effects of this polyphenol by improving endothelial function.

Keywords:
Calcium / Endothelial cells / Imaging / Nitric oxide / Resveratrol

1 Introduction

Trans-resveratrol (3,4′,5-trihydroxy-*trans*-stilbene; *t*-Resv) is a natural phenolic component of *Vitis vinifera* L. (Vitaceae), abundant in the skin of grapes and present in wines, especially red wines [1, 2]. It is not unique to *Vitis* but is also present in at least 72 other plant species, many of which are part of the human diet, such as *Morus alba* (mulberries) and *Arachis hypogaea* (peanuts) [3, 4].

t-Resv possesses biological properties that could have therapeutic relevance in the prevention of many cardiovascular diseases [5–8]. It relaxes the agonist-induced contractile

Correspondence: Professor Manuel Campos-Toimil, Departamento de Farmacoloxía, Facultade de Farmacia, Universidade de Santiago de Compostela, Campus Vida, E-15782 Santiago de Compostela, Spain
E-mail: manuel.campos@usc.es
Fax: +34-981594595

Abbreviations: AMPK, 5′ adenosine monophosphate-activated protein kinase; **DAF-2,** 4,5-diaminofluorescein; **eNOS,** endothelial nitric oxide synthase; **ERK1/2,** extracellular signal-regulated kinase 1/2; **HUVEC,** human umbilical vein endothelial cell; **L-NAME,** N^{ω}-nitro-L-arginine methyl ester hydrochloride; **L-NNA,** N^{ω}-nitro-L-arginine; **NO,** nitric oxide; **NSCC,** non-selective cation channel; **ROS,** reactive oxygen species; **SERCA,** sarcoplasmic/ER Ca^{2+}-ATPase; **SIRT1,** silent mating type information regulation 2 homolog; **SKF 96365,** 1-(β-[3-(4-methoxy-phenyl)propoxy]-4-methoxyphenethyl)-1H-imidazole hydrochloride; **SOCC,** store operated Ca^{2+} channels; **SOCE,** store-operated calcium entry; **TMB-8,** [3,4,5-trimethoxybenzoic acid 8-(diethylamino)octyl ester]; ***t*-Resv,** *trans*-resveratrol; **VOCCs,** voltage-operated Ca^{2+} channels; **VSMCs,** vascular smooth muscle cells

*Current address: Division of Cardiovascular and Neuronal Remodelling, Leeds Institute of Genetics, Health and Therapeutics, University of Leeds, Leeds LS2 9JT, UK
**In memoriam of Dr. Francisco Orallo.

response in endothelium-intact rat aorta at concentrations greater than 30 μM, an effect reversed by the competitive nitric oxide synthase inhibitor, N^{ω}-nitro-L-arginine (L-NNA). At higher concentrations (greater than 60 μM), *t*-Resv also relaxes endothelium-denuded aortic rings, but this effect cannot be reversed by L-NNA, suggesting that *t*-Resv exerts both nitric oxide (NO)-mediated and non-NO-mediated vasodilator effects [9]. We have previously reported that *t*-Resv exhibits endothelium-dependent and -independent relaxant responses in rat aorta; the former partly mediated by inhibition of vascular NADH/NADPH oxidase, resulting in attenuated cellular O_2^- generation and, therefore, NO biotransformation [8]. This endothelium-dependent component is observed at lower drug concentrations (1–10 μM) than the endothelium-independent effect (more than 50 μM) [8, 10]. A direct involvement of the endothelium in the vasorelaxant effect of *t*-Resv is also supported by other studies [11–14], although opposing results have been reported in rat pulmonary arteries [15]; for review see [6].

Other reports have also shown that *t*-Resv may increase NO availability by interfering with the generation of reactive oxygen species (ROS) [16, 17]. It has also been suggested that *t*-Resv enhances endothelial nitric oxide synthase (eNOS) activity via 5′ adenosine monophosphate-activated protein kinase (AMPK)- or extracellular signal-regulated kinase 1/2 (ERK1/2)-mediated phosphorylation at Ser^{1177} [18, 19]. Yet more mechanisms of action have been proposed but these become evident only after prolonged exposure to *t*-Resv: for example, activation of silent mating type information regulation 2 homolog (SIRT1) can promote direct deacetylation of eNOS [20]. Discussion of the diverse mechanisms proposed to explain how *t*-Resv might enhance endothelial activity and NO production can be found at greater depth in [17].

Concerning Ca^{2+} handling in the vascular effects of *t*-Resv, we have reported that vasorelaxation in rat aortic rings is not mediated by blockade of Ca^{2+} influx through receptor-operated calcium channels [10]. Other groups have suggested that *t*-Resv may reduce Ca^{2+} influx through voltage-operated Ca^{2+} channels (VOCCs) or Ca^{2+} release from intracellular stores in vascular smooth muscle cells (VSMCs) [11] and ventricular myocytes [21, 22]. More recently, we have demonstrated that both *trans*- and *cis*-resveratrol block L-type VOCCs in rat aortic myocytes [23]. Surprisingly, in this same cell type, resveratrol isomers may also induce a sustained elevation in basal $[Ca^{2+}]_c$ by depleting Ca^{2+} from intracellular stores and subsequently initiating store-operated Ca^{2+} entry, although the possibility of influx via another type of Ca^{2+} channels cannot be discounted [23, 24]. A similar effect of *t*-Resv in endothelial cells could then induce an increase in the biosynthesis and release of NO, since it has been reported that substances that increase endothelial $[Ca^{2+}]_c$ potentially influence the production of endothelial factors, notably NO, because of the Ca^{2+} sensitivity of eNOS in the endothelium [25, 26].

In view of these reports, we hypothesised that a *t*-Resv-induced increase in $[Ca^{2+}]_c$ in endothelial cells leads to an elevated NO production. To investigate this proposal, we separately and simultaneously recorded Ca^{2+} and NO levels in human umbilical vein endothelial cells (HUVECs) by using fura-2 and 4,5-diaminofluorescein (DAF-2). We also tested the effect of *t*-Resv in an in vitro NO production assay using recombinant bovine eNOS. Our results indicate that *t*-Resv induces a concentration-dependent, simultaneous increase in both $[Ca^{2+}]_c$ and NO release in human endothelial cells. The NO rise depends almost exclusively on the $[Ca^{2+}]_c$ increase, although a direct activation of ERK1/2 and AMPK pathways might contribute. Together, our observations provide the basis for a simple model to explain the endothelium-dependent vasorelaxant property of this natural dietary polyphenol.

2 Materials and methods

2.1 Cell culture

HUVEC (HUVEC-C, a spontaneously transformed cell line) were purchased from American Type Culture Collection (ATCC 1730-CRL; Rockville, MD, USA). This cell line is a pure population of cells that preserve established endothelial cells characteristics [27]. The cells were grown in Kaighn's F12K medium containing L-glutamine (2 mM), sodium bicarbonate (1.5 g/L), endothelial cell growth supplement (0.03 mg/mL), heparin (0.1 mg/mL), antibiotics/antimycotic (100 units/mL penicillin, 100 μg/mL streptomycin and 0.25 μg/mL amphotericin B) and 10% v/v heat-inactivated foetal bovine serum. Cells were maintained at 37°C with 5% CO_2 in air and used for experimentation between passages 10 and 25. The passage number did not alter cell response.

For imaging experiments in isolated cells, HUVECs were seeded at ~1500 cells/cm^2 in 35 mm Petri dishes in which a 20 mm diameter hole had been cut in the base and replaced by a 0.1 mm glass coverslip. Cells were allowed to grow for at least 24 h in culture medium.

For experiments using HUVEC monolayers, cells were seeded in 96-well plates (50 000 cells/cm^2) and kept in culture (37°C, 5% CO_2 in air) for exactly 48 h to ensure equivalent density in all wells.

2.2 $[Ca^{2+}]_c$ imaging in isolated HUVECs

HUVECs were incubated for 60 min at 37°C in normal bathing solution (composition in mM: NaCl 140, KCl 5, $CaCl_2 \cdot 2H_2O$ 1.5, $MgCl_2$ 2, HEPES 10, glucose 11, pH 7.4) containing fura-2 acetoxymethyl ester (2.5 μM), a cell membrane-permeable Ca^{2+}-sensitive fluorescent dye [28]. Cells were then gently washed twice with normal bathing solution and allowed to rest for >15 min in the incubator, to allow the hydrolysis of fura-2 acetoxymethyl ester into the free Ca^{2+}-sensitive free acid form (fura-2) by cell esterases.

Cells were placed on an Axiovert 135 inverted light microscope (Zeiss, Oberkochen, Germany) and continuously perfused at 0.5 mL/min with normal bathing solution except

during the application of drugs. For experiments in extracellular Ca^{2+}-free medium, $CaCl_2$ was replaced by EGTA (1 mM). Measurements were made from isolated cells viewed with a Plan-Neofluar, $63\times/1.25$ oil immersion objective (Zeiss) using a digital imaging system. Fura-2 was excited alternately at 340 ± 10 nm and 380 ± 10 nm (100 ms exposure time for both wavelengths) using an XBO 75W/2 xenon lamp (Zeiss). Excitation light from the P130/MLE/400 Optoscan monochromator (Cairn Research, Faversham, UK) was reflected by a dichroic mirror with a half-pass wavelength of 400 nm. Emitted fluorescence was collected through a 510 ± 20 nm emission filter and measured with an intensified charge-coupled device camera (C651-ICCD, Cairn Research). Ratiometric Ca^{2+} images were generated at 2–10 s intervals, using four averaged images at each wavelength. Images were digitally stored and analysed using the MetaFluor software (Universal Imaging, West Chester, PA, USA).

For incubation periods, drugs (or vehicle controls) were added in volumes of 0.5–10 μL to a final incubation volume of 1 mL of bathing solution.

All procedures and experiments were performed at room temperature to minimise compartmentalisation and cell extrusion of the fluorescent dye.

2.3 Simultaneous measurement of intracellular NO and $[Ca^{2+}]_c$

HUVECs were kept in culture with culture medium containing L-arginine (100 μM) for 24 h. They were then incubated for 60 min at 37°C in normal bathing solution containing fura-2 AM (2.5 μM) and DAF-2 diacetate (5 μM), a cell membrane-permeable NO-sensitive fluorescent dye [29], and treated as for $[Ca^{2+}]_c$ imaging experiments.

Cells loaded with both fluorescent probes were excited alternately as described above for fura-2 imaging and additionally at 490 ± 10 nm (200 ms exposure time) for DAF-2 imaging. A dichroic mirror reflected short-wave (<500 nm) fluorescence, but permitted long-wave fluorescence to pass. Emitted fluorescence was collected through a 510 ± 20 nm emission filter. Ratiometric Ca^{2+} images and NO images were generated at 10 s intervals, using four averaged images at each wavelength, and digitally stored for later analysis with the MetaFluor software.

2.4 Determination of NO release from HUVEC monolayers

Confluent HUVEC in 96-well plates were washed twice with PBS (composition in mM: 137 NaCl, 2.7 KCl, 0.5 $MgSO_4\cdot7H_2O$, 0.9 $CaCl_2\cdot2H_2O$, 1.5 KH_2PO_4; pH 7.4). Cells were then incubated in PBS containing L-arginine (100 μM) for 10 min at 37°C. After that, HUVECs were treated for 20 min with PBS containing Ni^{2+}, 1-(β-[3-(4-methoxy-phenyl)propoxy]-4-methoxyphenethyl)-1H-imidazole hydrochloride (SKF 96365), [3,4,5-trimethoxybenzoic acid 8-(diethylamino)octyl ester] (TMB-8), N^{ω}-nitro-L-arginine methyl ester hydrochloride (L-NAME), SIRT1 inhibitor III, PD98079, dorsomorphin or vehicle. Subsequently, HUVECs were incubated in PBS containing DAF-2 (0.1 μM). This low concentration of DAF-2 was chosen in order to reduce the contribution of DAF-2 auto-fluorescence (measured in wells without cells), which was subtracted from the measured total fluorescence, according to the experimental protocol previously detailed by Räthel et al. [30]. This method allows the quantification of NO in human endothelial cells in the nanomolar range.

Under these conditions, *t*-Resv, thapsigargin, ionomycin or vehicle (controls) were added to the corresponding well plates. In some experiments, the NO donor sodium nitroprusside was used as a positive control for the technique. Then, the fluorescence of supernatants was measured every 10 min for 40 min at room temperature using a Titertek Multiskan PLUS MKII multi-well plate reader (Titertek, Huntsville, AL, USA). The excitation and emission wavelengths were 490 and 515 nm, respectively.

2.5 Determination of in vitro eNOS activity

Production of NO from recombinant bovine eNOS was measured using DAF-2 and FCANOS1, a fluorimetric NO detection system that provides an optimal buffer containing cofactors and divalent cations essential for enzyme activity. Two different solutions were prepared for each assay: reaction buffer (25 mM Tris, 1 μM β-NADPH, 0.2 μM calmodulin, 6 μM tetrahydro-biopterin, 2 μM flavin mononucleotide, 2 μM flavin adenine dinucleotide, 2 mM $CaCl_2$; pH 7.4) and DAF-2 solution (25 mM Tris, 1 μM DAF-2, 0.1×10^{-3} units/well recombinant eNOS and varying concentrations of *t*-Resv; pH 7.4).

Aliquots of 50 μL of each solution were added in triplicate to clear-bottom black 96-well plates. Plates were incubated for 15 min in the absence of any light, at room temperature. Fluorescence was measured in a multi-well plate reader (FLUOstar OPTIMA; BMG Labtech, Offenburg, Germany) before (time zero) and after (every 3 s for 15 min) adding L-arginine (100 μM) through on-board reagent injectors. The excitation and emission wavelengths were 485 and 520 nm, respectively.

A number of experimental controls were performed, including addition of the eNOS inhibitor L-NNA (100 μM) and inactivation of eNOS by boiling prior to the experiment. Also, reactions omitting either NADPH, Ca^{2+}, or fluorescent probe were performed.

2.6 Drugs, chemicals and media

Antibiotics/antimycotic (penicillin G, streptomycin and amphotericin B), DMSO, FCANOS1 kit for detection of eNOS activity, heparin, ionomycin, L-arginine hydrochloride,

L-glutamine, L-NAME, L-NNA, SKF 96365, TMB-8 and *t*-Resv were purchased from Sigma-Aldrich. (St. Louis, MO, USA). Thapsigargin was from RBI (Natick, MA, USA). Dorsomorphin (6-[4-(2-piperidin-1-ylethoxy)phenyl]-3-pyridin-4-ylpyrazolo[1,5-a]pyrimidine; compound C), PD98059 (2′-amino-3′-methoxyflavone) and SIRT1 inhibitor III (6-chloro-2,3,4,9-tetrahydro-1H-carbazole-1-carboxamide) were from Calbiochem (Darmstadt, Germany). Kaighn's F12K medium was from ATCC. Endothelial cell growth supplement was from Upstate (Lake Placid, NY, USA). Foetal bovine serum was from Gibco-Life Technologies (Grand Island, NY, USA). Fura-2 acetoxymethyl ester was from Molecular Probes (Eugene, OR, USA). DAF-2 and DAF-2 diacetate were from Cayman Chemical (Ann Arbor, MI, USA). All other reagents were of analytical grade.

Stock solutions of the following compounds were prepared and stored at −20°C as follows: $LaCl_3 \cdot 7H_2O$ (50 mM), L-arginine (100 mM), L-NAME (10 mM), L-NNA (10 mM), Ni^{2+} (10 mM), SKF 96365 (10 mM) and TMB-8 (10 mM) in distilled water; dorsomorphin (10 mM), ionomycin (1 mM), PD98059 (10 mM), SIRT1 inhibitor III (10 mM), *t*-Resv (100 mM) and thapsigargin (1 mM) in DMSO.

From these stock solutions, dilutions in physiological buffer were freshly prepared for each experiment. Fura-2-AM (2.5 μM) was prepared daily in physiological buffer containing 0.1% DMSO. DAF-2 and DAF-2 diacetate were diluted daily in physiological buffer from a commercial solution (1.38 and 1.12 mM, respectively) in 100% DMSO. The final concentration of DMSO never exceeded 0.1%.

Appropriate cautionary measures were taken throughout the procedure to avoid degradation of light-sensitive resveratrol and extensive photobleaching of the fluorescent dyes. The pH of all solutions was carefully measured before the start of each experiment since fluorescence of DAF derivatives is highly pH dependent [30].

2.7 Data presentation and statistical analysis

Unless otherwise stated, the results shown in the text and figures are expressed as mean ± SEM. Significant differences between two means ($p<0.05$ or $p<0.01$) were determined by Student's two-tailed *t* test for paired or unpaired data or by one-way analysis of variance followed by Bonferroni's post hoc test, when appropriate.

For each isolated HUVEC, the fluorescence emitted was averaged from pixels within manually outlined cell areas. Background compensation was performed by subtracting the illumination from an area of the image which contained no cells. For the determination of NO release from HUVEC monolayers, the auto-fluorescence of DAF-2 was measured from a group of well plates containing no cells.

The $[Ca^{2+}]_c$ was then calculated from the 340/380 nm fluorescence ratio as described by Grynkiewicz et al. [28]. Ratios were converted into free Ca^{2+} by the equation: $[Ca^{2+}]_c = K_d\ (R\text{-}R_{min}/R_{max}\text{-}R)\ (F_{min380}/F_{max380})$, where K_d is the affinity constant of fura-2 for Ca^{2+}, R is the 340/380 nm fluorescence ratio, R_{min} and R_{max} are the limiting ratios for minimal (0 mM Ca^{2+} and 10 mM EGTA in the bath) and saturating $[Ca^{2+}]_c$ (10 mM Ca^{2+} in the bath) both in the presence of ionomycin (10 μM). F_{min380}/F_{max380} is the ratio of fluorescence of fura-2 at 380 nm in the presence of minimal to that of saturating $[Ca^{2+}]_c$.

Basal $[Ca^{2+}]_c$ was determined by averaging resting Ca^{2+} values measured for 10 s on cells from different preparations. Maximal increases in $[Ca^{2+}]_c$ were calculated by subtracting basal values from the maximal $[Ca^{2+}]_c$ achieved for each individual cell. In experiments with isolated HUVECs, only data obtained from cells that responded to the Ca^{2+} ionophore ionomycin (0.5 μM), in the presence of external $CaCl_2$ (1.5 mM), at the end of the experiments, were used. From the cumulative-response curves, the 50% effective concentration (EC_{50}) for the effect of *t*-Resv was determined by graphical estimation from a best fit concentration response curve. For imaging experiments, the number "*n*" represents the number of single cells from the same cell culture corresponded to passages 10–25.

3 Results

3.1 Effects of *t*-Resv on basal $[Ca^{2+}]_c$

In external solution containing 1.5 mM Ca^{2+}, mean basal $[Ca^{2+}]_c$ in HUVECs was 76.7 ± 4.3 nM ($n = 16$), which did not change throughout the experimental time course. Cumulative application of *t*-Resv (0.3–60 μM) induced a sustained increase in $[Ca^{2+}]_c$ in HUVECs (maximal increase in $[Ca^{2+}]_c$: 152.3 ± 11.2 nM, $EC_{50} = 37.1 \pm 1.8$ μM, $n = 16$, $p<0.01$ with respect to control; see representative trace in Fig. 1). The percentage of endothelial cells that showed an increase in $[Ca^{2+}]_c$ was ∼75%.

In a Ca^{2+}-free external solution, the average basal $[Ca^{2+}]_c$ was 70.9 ± 3.1 nM ($n = 44$, $p>0.05$ with respect to 1.5 mM Ca^{2+} external solution), and was unchanged throughout the experimental time course. Under these conditions, 60% of the cells responded to the application of *t*-Resv (30 μM) with a rise in $[Ca^{2+}]_c$ that reached a maximum at ∼10 min before returning to basal values after ∼25 min (maximal increase: 79.2 ± 6.5 nM, $n = 21$, $p<0.01$ with respect to control; Fig. 2C). This response was not present after depletion of intracellular Ca^{2+} stores with thapsigargin (0.5 μM), which itself induced a transient increase in $[Ca^{2+}]_c$ (maximal increase: 160.4 ± 12.0 nM, $n = 9$, $p<0.01$ with respect to the *t*-Resv-induced increase; Fig. 2A and C). The rise in $[Ca^{2+}]_c$ evoked by thapsigargin was significantly reduced after partial depletion of intracellular Ca^{2+} stores with 30 μM *t*-Resv (maximal $[Ca^{2+}]_c$: 77.3 ± 9.3 nM, $n = 12$; $p<0.01$ with respect to values in the absence of *t*-Resv; Fig. 2B and C).

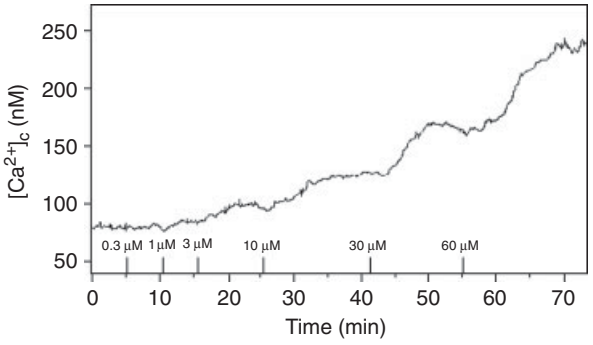

Figure 1. *t*-Resv mobilises $[Ca^{2+}]_c$ in HUVECs. Representative trace of the cumulative increases in $[Ca^{2+}]_c$ induced by *t*-Resv (0.3–60 μM) in fura-2-loaded isolated cells in a 1.5 mM Ca^{2+}-containing external solution.

After the $[Ca^{2+}]_c$ elevation induced by a single application of *t*-Resv or thapsigargin, replacement of Ca^{2+}-free with a calcium-containing solution (1.5 mM $CaCl_2$), induced an increase in $[Ca^{2+}]_c$ (maximal increase in $[Ca^{2+}]_c$: 117.0 ± 14.1 nM, $n = 15$ and 188.6 ± 9.9 nM, $n = 10$, for *t*-Resv and thapsigargin, respectively; Fig. 3) due to store-operated calcium entry (SOCE) following the classic model of the capacitative Ca^{2+} entry pathway, a process whereby the emptying of intracellular Ca^{2+} stores provokes the activation of store-operated plasma membrane Ca^{2+} channels [31]. The capacitative Ca^{2+} entry inhibitor Ni^{2+} (300 μM), the non-selective Ca^{2+} inhibitor SKF 96365 (30 μM) and La^{3+} (500 μM), a blocker of VOCCs and SOCEs, significantly decreased both *t*-Resv- and thapsigargin-induced SOCE (Fig. 3B). Pre-incubation with these ion channel blockers did not change the maximal increase in $[Ca^{2+}]_c$ induced by *t*-Resv and thapsigargin (data not shown).

3.2 *t*-Resv-induced $[Ca^{2+}]_c$ increase leads to NO release in HUVECs

Having characterised the effects of *t*-Resv on Ca^{2+} mobilisation, we next explored a potential link to the NO pathway by monitoring $[Ca^{2+}]_c$ and intracellular NO levels in the same cell. In external solution containing 1.5 mM Ca^{2+}, three distinct responses of HUVECs to application of *t*-Resv (30 μM) were observed (Table 1). Firstly, in ~30% of cells, *t*-Resv induced an increase in $[Ca^{2+}]_c$ with a transient and a sustained component (Table 1; see representative traces in Fig. 4). In this group, a simultaneous increase in NO biosynthesis (~25% of the increase in NO biosynthesis induced by 0.5 μM ionomycin) was measured. NO levels started to increase ~1–3 s after the maximum peak in $[Ca^{2+}]_c$ was reached. Second, in ~50% of cells, *t*-Resv induced a slow and sustained rise in $[Ca^{2+}]_c$ (Table 1). In this case, there was not a significant increase in NO biosynthesis. Finally, and in contrast to the preceding two

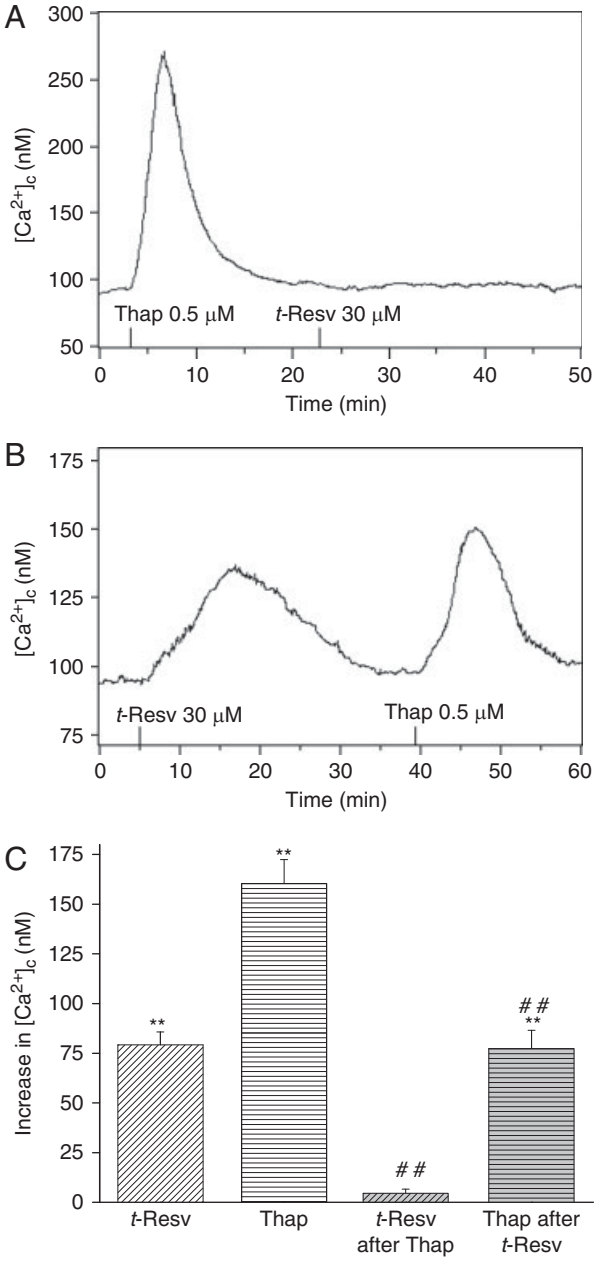

Figure 2. *t*-Resv acts by mobilizing thapsigargin-sensitive intracellular Ca^{2+} stores in HUVECs. Representative trace illustrating that the increase in $[Ca^{2+}]_c$ induced by *t*-Resv (30 μM) in the absence of extracellular Ca^{2+} was completely abolished after depletion of intracellular Ca^{2+} stores with thapsigargin (Thap, 0.5 μM) (A), and that the thapsigargin-induced $[Ca^{2+}]_c$ rise was significantly lower after an application of *t*-Resv (B). (C) Average data from at least nine cells per experiment showing the reciprocal interference between the increases in $[Ca^{2+}]_c$ induced by *t*-Resv (30 μM) and thapsigargin (Thap, 0.5 μM) in the absence of extracellular Ca^{2+}. $^{**}p < 0.01$ versus basal values and $^{\#\#}p < 0.01$ versus the corresponding value in the absence of *t*-Resv or thapsigargin.

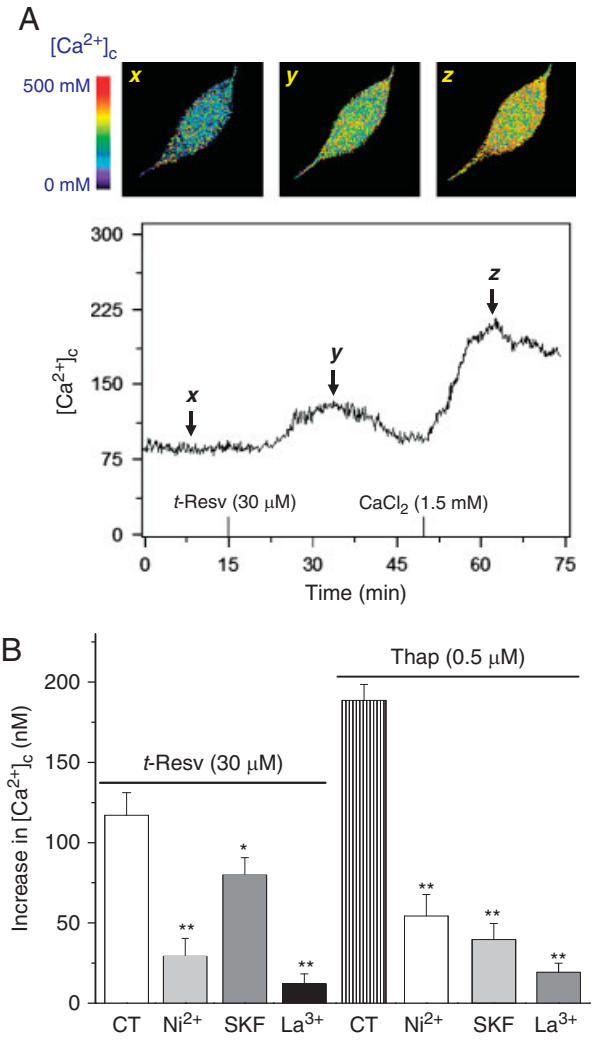

Figure 3. *t*-Resv induces Ca^{2+} influx in HUVECs. (A) Representative trace and corresponding fura-2 digital images at three different time-points (*x*, *y* and *z*) of the increase in $[Ca^{2+}]_c$ induced by *t*-Resv in a Ca^{2+}-free solution and the subsequent capacitative Ca^{2+} entry measured after reintroduction of external Ca^{2+} (1.5 mM). (B) Average data from at least nine cells per treatment showing the effects of Ni^{2+} (300 μM) SKF 96365 (SKF; 30 μM) or La^{3+} (500 μM) on the SOCE induced by *t*-Resv and thapsigargin (Thap). $^{*}p<0.05$ and $^{**}p<0.01$ versus control values (CT).

Table 1. $[Ca^{2+}]_c$ responses and NO release induced by *t*-Resv in HUVECs

	% of cells (*n*)	Maximal $[Ca^{2+}]_c$ increase (nM)	Increase in NO levels (% of response to ionomycin)
T+S	28.6 (18)	$272.7 \pm 12.7^{a)}$(T) $108.2 \pm 9.3^{a)}$ (S)	$23.8 \pm 5.4^{b)}$
S	49.2 (31)	$108.7 \pm 12.0^{a)}$	5.3 ± 2.8
NR	22.2 (14)	–	–

T+S, transient + sustained: cells that exhibit both transient and sustained components of the increase in $[Ca^{2+}]_c$ induced by *t*-Resv (30 μM). S, sustained: cells that only display the slow sustained component of the *t*-Resv-induced $[Ca^{2+}]_c$ increase. NR, no response: cells that do not show an increase in $[Ca^{2+}]_c$ in response to *t*-Resv.

a) Level of statistical significance: $p<0.01$ with respect to control.

b) $p<0.05$ with respect to basal NO levels.

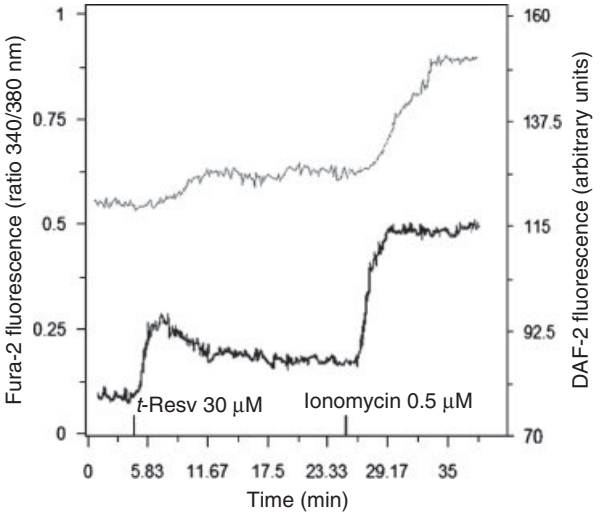

Figure 4. *t*-Resv induces both increase of $[Ca^{2+}]_c$ and NO bioavailability in HUVECs. Original traces showing the simultaneous increases in $[Ca^{2+}]_c$ (black) and NO (grey) induced by a single application of *t*-Resv followed by a single application of ionomycin in an isolated HUVEC in the presence of 1.5 mM external Ca^{2+}.

responses, ~20% ($n = 14$) of cells were refractory to the application of *t*-Resv (Table 1), despite exhibiting significantly increased $[Ca^{2+}]_c$ and NO biosynthesis after subsequent challenge with 0.5 μM ionomycin (data not shown).

In the presence of La^{3+} (500 μM), *t*-Resv evoked an increase in $[Ca^{2+}]_c$ in ~60% of the cells, which was significantly lower than in the absence of La^{2+} (maximal increase in $[Ca^{2+}]_c$: 87.2 ± 8.5 nM, $n = 19$, $p<0.01$ with respect to the increase in the absence of La^{3+}). Under these conditions, none of the cells displayed measurable increases in NO.

3.3 *t*-Resv increases NO release in HUVEC monolayers

To confirm and complement our measured NO increase in single cells, we then investigated responses of HUVEC populations to *t*-Resv. The NO donor sodium nitroprusside (100 μM) and the Ca^{2+} ionophore ionomycin (0.5 μM) evoked significant increases in NO release. The application of *t*-Resv (30, 60 μM) or thapsigargin (0.5 μM) to HUVEC monolayers induced a concentration-dependent increase in

NO release, which was maximal at 10 min post-treatment. A lower concentration of *t*-Resv (1 μM) did not produce an effect (Fig. 5A).

The increase in NO release induced by *t*-Resv (30 or 60 μM) was partially inhibited by SKF 96365 (30 μM) and Ni^{2+} (300 μM) and completely abolished by TMB-8 (100 μM) (Fig. 5B). L-NAME (500 μM) also completely inhibited the rise in NO (data not shown).

As noted in the introduction, *t*-Resv has been reported to enhance eNOS activity via AMPK, ERK or SIRT1 in HUVECs. In order to explore the dependence of *t*-Resv on SIRT1, ERK1/2 and AMPK for its effects in HUVECs, we performed experiments using selective inhibitors of these enzymes (SIRT1 inhibitor III, PD98059 and dorsomorphin, respectively).

The stimulation of NO release induced by *t*-Resv (60 μM) was only partially reduced by 20 min incubation with both PD 98059 (50 μM) or dorsomorphin (20 μM). SIRT1 inhibitor III (5 μM) had no effect on the *t*-Resv-induced NO release (Fig. 5C).

3.4 *t-Resv* does not directly activate eNOS in vitro

The data presented so far strongly indicate activation of Ca^{2+} and NO signalling pathways in HUVECs. As highlighted in the introduction, *t*-Resv might act on a number of Ca^{2+} channels. We were therefore interested in whether *t*-Resv could directly activate eNOS. For this, we chose a simple in vitro assay of eNOS activity, using purified bovine eNOS and DAF-2. As shown in Fig. 6, the nitric oxide synthase substrate L-arginine (100 μM) induced a significant fivefold increase in basal DAF-2 fluorescence. The level of eNOS activity in the presence of L-arginine was not modified by preincubation with *t*-Resv (0.5–100 μM). Application of the NO donor sodium nitroprusside (100 μM) increased basal from 1020.5 ± 20.0 to 2370.6 ± 14.3 units, demonstrating that the DAF-2 signal was not saturated (data not shown). Basal eNOS activity was blocked by preincubation with L-NNA (100 μM). Taken together these data suggest that *t*-Resv does not directly stimulate eNOS.

3.5 Inhibition of AMPK or ERK1/2, but not SIRT1, reduces *t*-Resv-induced NO production without modifying *t*-Resv-induced rises in $[Ca^{2+}]c$ in isolated HUVECs

Since AMPK or ERK1/2 inhibition reduced *t*-Resv-evoked NO rises measured in HUVEC monolayers, we decided to simultaneously monitor Ca^{2+} mobilisation and NO levels induced by *t*-Resv in the presence of dorsomorphin or PD98059 in single cells. The aim of these experiments was to investigate whether AMPK or ERK1/2 inhibition had an effect on $[Ca^{2+}]_c$ rises, which seem to underlie the *t*-Resv-stimulated increase NO bioavailability.

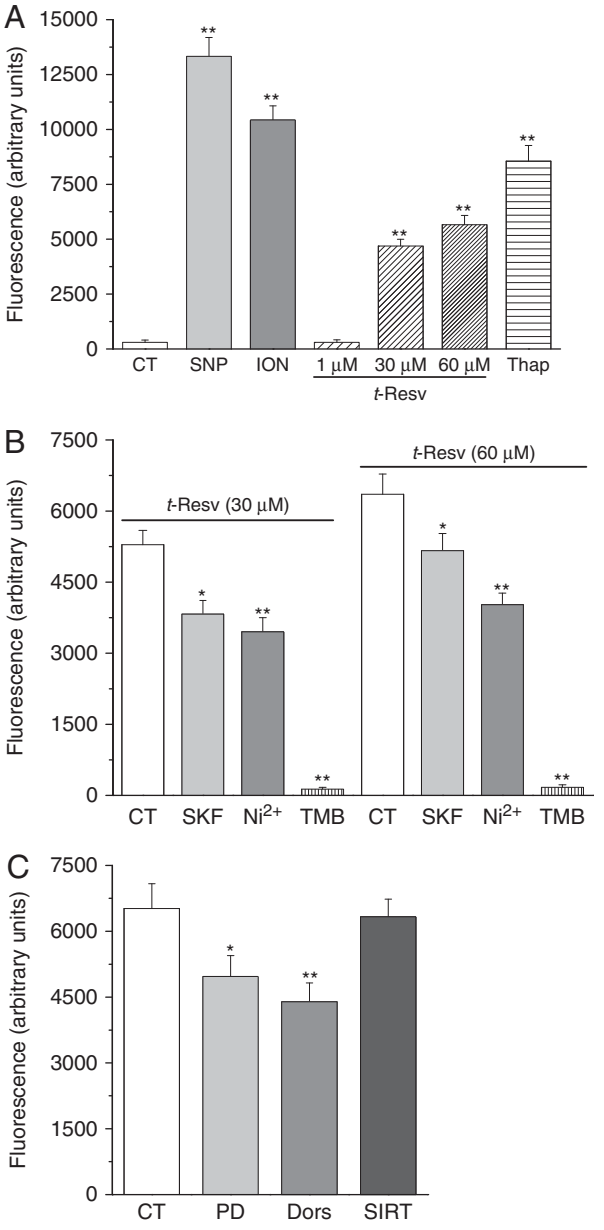

Figure 5. Effects of *t*-Resv on NO release in HUVEC cells. (A) Increases in DAF-2 fluorescence (indicative of NO release) measured after 10 min of incubation with sodium nitroprusside (100 μM), ionomycin (0.5 μM), *t*-Resv (30, 60 μM) and thapsigargin (Thap; 0.5 μM) and lack of effects of *t*-Resv (1 μM). (B) Reduction of the *t*-Resv-induced increases in NO by SKF 96365 (SKF, 30 μM), Ni^{2+} (300 μM) and TMB-8 (TMB; 100 μM). (C) Effects of PD98059 (PD; 50 μM), dorsomorphin (Dors; 20 μM) or SIRT1 inhibitor III (SIRT; 5 μM) on the increases in NO induced by *t-Re*sv (60 μM). Each bar represents the mean ± SEM (indicated by vertical lines) of at least ten experiments. $^{*}p<0.05$ or $^{**}p<0.01$ versus control values (CT).

Dorsomorphin or PD98059 did not alter *t*-Resv-induced rises in $[Ca^{2+}]_c$ in either of the two types of responses we observed in single cells: transient plus sustained, and sustained only (Table 2). *t*-Resv-evoked NO rises were,

however, reduced to a significant extent in cells treated with dorsomorphin.

On the other hand, SIRT1 inhibitor III did not significantly modify *t*-Resv- and ionomycin-induced responses.

4 Discussion

In the present study, *t*-Resv concentration-dependently increased $[Ca^{2+}]_c$ in HUVEC. In ~30% of the cells, the increase induced by a single concentration of *t*-Resv consisted of a transient phase followed by a sustained plateau, while in ~50% only the plateau phase was observed.

In the absence of extracellular Ca^{2+}, *t*-Resv also augmented $[Ca^{2+}]_c$, an effect that was abolished after depletion of intracellular Ca^{2+} stores by inhibition of the sarcoplasmic/ER Ca^{2+}-ATPase (SERCA) with thapsigargin. Also in a Ca^{2+}-free extracellular solution, the thapsigargin-evoked increase in $[Ca^{2+}]_c$ was reduced by ~50% after a calcium response to *t*-Resv. Furthermore, depletion of intracellular Ca^{2+} stores with *t*-Resv or thapsigargin activates SOCE, which can be significantly inhibited by the non-selective Ca^{2+} channel blockers Ni^{2+}, SKF 96365 or La^{3+}. These results suggest that the *t*-Resv-induced $[Ca^{2+}]_c$ rise is mediated by a release of Ca^{2+} from thapsigargin-sensitive intracellular stores and the subsequent SOCE through store operated Ca^{2+} channels (SOCC), although a direct activation of other plasma membrane Ca^{2+} channels, such as non-selective cation channels (NSCCs) may be also implicated.

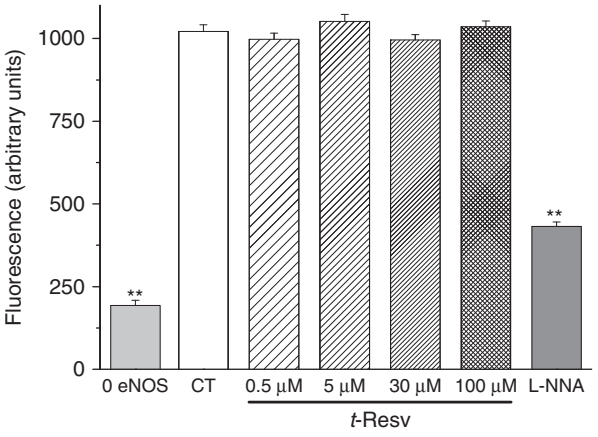

Figure 6. *t*-Resv does not affect recombinant bovine eNOS activity in vitro. Basal DAF-2 fluorescence without eNOS (0 eNOS), eNOS activity after addition of 100 μM L-arginine in the absence (CT) or in the presence of *t*-Resv (0.5–100 μM) or L-NNA (100 μM). Each bar represents mean ± SEM of ten independent experiments $^{**}p<0.01$ versus control values.

We have previously reported that both *trans*- and *cis*-resveratrol elicit an increase in $[Ca^{2+}]_c$ in VSMC [23, 24]. This $[Ca^{2+}]_c$ increase was mainly mediated by depletion of Ca^{2+} from intracellular stores sensitive to thapsigargin, and subsequent influx of Ca^{2+} through SOCC but also by another type of Ca^{2+}-permeable channel that was not affected by Ni^{2+}, nifedipine or SKF 96365. In light of those results obtained in VSMC and the results presented in this work with endothelial cells, it is likely that *t*-Resv inhibits the action of SERCA. This supposition is supported by previously published work describing inhibition of ATPase activity by *t*-Resv [32, 33].

Our imaging experiments combining Ca^{2+}- and NO-sensitive dyes have shown that there is a significant increase in NO biosynthesis immediately after commencement of the *t*-Resv-induced increase in $[Ca^{2+}]_c$. This effect was observed strictly in those cells in which the nature of the $[Ca^{2+}]_c$ rise was biphasic (peak and plateau). However, in the presence of La^{3+}, which markedly inhibits SOCE (see above), the increase in $[Ca^{2+}]_c$ was significantly reduced and the increase in NO completely abolished.

In experiments using DAF-2 in HUVEC monolayers, *t*-Resv induced a significant increase in NO release that was abolished by TMB-8, an inhibitor of intracellular Ca^{2+}

Table 2. Effects of the inhibition of AMPK with dorsomorphin (20 μM), ERK1/2 with PD98059 (30 μM) and SIRT1 with SIRT1 inhibitor III (5 μM) on the increase in $[Ca^{2+}]_c$ (nM) and NO release (expressed as % of the response evoked by 0.5 μM ionomycin) induced by *t*-Resv (30 μM)

	Control	PD98059	Dorsomorphin	$SIRT_1$ inhibitor III
T+S (% of cells)	25.6	22.5	23.6	25.5
$[Ca^{2+}]$ Transient	298.7 ± 15.1[a)]	257.3 ± 22.7[a)]	277.9 ± 19[a)]	286.9 ± 10.0[a)]
$[Ca^{2+}]$ Sustained	115.9 ± 10.2[a)]	103.8 ± 23.4[a)]	101.9 ± 11.2[a)]	109.9 ± 12.1[a)]
NO increase	21.8 ± 5.8[a)]	13.2 ± 3.4[a)b)]	12.9 ± 2.6[a)c)]	23.2 ± 6.1[a)]
S (% of cells)	48.8	47.6	45.7	50.3
$[Ca^{2+}]$ increase	109.4 ± 12.8[a)]	103.4 ± 15.4[a)]	114.3 ± 14.5[a)]	112.4 ± 8.5[a)]
NO increase	3.2 ± 1.0	4.7 ± 1.6	2.3 ± 0.9	4.0 ± 1.7

T+S, transient + sustained: cells that exhibit both transient and sustained components of the increase in $[Ca^{2+}]_c$. S, sustained: cells that only display the slow sustained component of the *t*-Resv-induced $[Ca^{2+}]_c$ increase.
a) Level of statistical significance: $p<0.01$ with respect to basal NO or $[Ca^{2+}]_c$ levels.
b) $p<0.01$
c) $p<0.05$ with respect to the corresponding control values; $n\geq 12$.

release that reduces Ca^{2+} availability by stabilizing Ca^{2+} binding to cellular Ca^{2+} stores [24, 34], thus supporting the hypothesis that depletion of intracellular Ca^{2+} is directly involved. The *t*-Resv-induced NO release was significantly reduced in the presence of Ni^{2+} and SKF 96365, which both have been shown to reduce SOCE in VSMC [24] and HUVEC [35].

These results suggest that in cells in which *t*-Resv induces a fast increase in $[Ca^{2+}]_c$ by depletion of intracellular stores and subsequent activation of SOCE, activation of NO release is high enough to be measured with our protocol. This is supported by the observation that substances that increase endothelial $[Ca^{2+}]_c$ potentially influence the biosynthesis of endothelial factors, notably NO, because of the Ca^{2+} sensitivity of eNOS in the endothelium [25, 26]. Furthermore, it has been reported that sustained NO release in HUVECs is highly dependent on store-operated Ca^{2+} entry [36, 37].

The increase of NO by *t*-Resv may be also related to its proven antioxidant properties. *t*-Resv reduces ROS generation, mainly $O_2^{-\cdot}$, through inhibition of NADH/NADPH oxidase activity. Such an effect decreases NO biotransformation [16]. However, it has been also shown that O_2^- induces an increase in $[Ca^{2+}]_c$ in human endothelial cells, which stimulates eNOS and counteracts NO inactivation [38]. The effects of O_2^- on Ca^{2+} handling in porcine aortic endothelial cells have been studied in detail by Graier et al. [39]. Further studies are needed to investigate the relative contribution of reduced ROS generation to the *t*-Resv-evoked increase in NO production and release described here.

In agreement with our results, Wallerath et al. [40] have measured a significant increase in NO release after short-term (2 min) treatment of HUVEC-derived EAA.hy926 cells with *t*-Resv (0.1–100 μM). However, most studies on the effects of *t*-Resv in NO production have been conducted with long-term experiments, in which the *t*-Resv-induced increase of NO is linked to enhanced eNOS expression [40–42]. In the same type of long-term experiments, dietary *t*-Resv has been shown to increase plasma NO levels in hypercholesteremic rabbits [43].

Nevertheless, the effects observed in the present study account for the short-term actions of *t*-Resv. The fact that PD98059 partially decreases NO production, without modifying $[Ca^{2+}]_i$ increases elicited by *t*-Resv suggests that ERK1/2 could mediate, at least in part, such a short-term effect. In accordance with this, Klinge et al. [18] have reported that *t*-Resv activates eNOS by phosphorylation mediated by oestrogen receptor signalling via ERK1/2. Similarly, inhibition of AMPK did not modify the increase in $[Ca^{2+}]_i$ elicited by *t*-Resv, but it reduced the *t*-Resv-induced increase in NO bioavailability, suggesting that this kinase might be also implicated in the activation of eNOS induced by *t*-Resv, as reported by Xu et al. [19].

On the other hand, although many studies have implicated SIRT1 in several actions mediated by *t*-Resv, we have found no relation of this sirtuin with the relatively fast increase in $[Ca^{2+}]_c$ and NO described here, since no significant differences were observed on these responses induced by *t*-Resv alone compared to those responses obtained with *t*-Resv in the presence of SIRT1 inhibitor III.

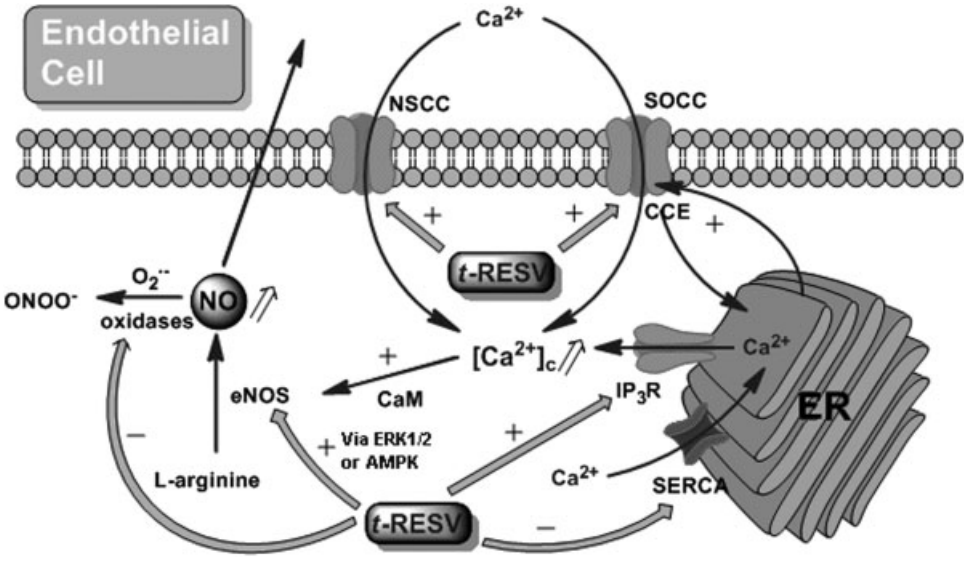

Figure 7. Simplified diagram of the proposed signalling events accounting for the effects of *t*-Resv on Ca^{2+} mobilisation and NO release in endothelial cells. *t*-Resv (30–60 μM) induces $[Ca^{2+}]_c$ rises by Ca^{2+} release from the ER, probably by inhibition of SERCA and/or activation of IP_3R; and Ca^{2+} influx through SOCC and NSCC. This fast increase in $[Ca^{2+}]_c$ favours Ca^{2+}-CaM binding which leads to potentiation of eNOS activity. Other mechanisms that contribute to short-term *t*-Resv-induced increase in NO bioavailability showed here are inhibition of oxidases and direct activation ERK1/2 and AMPK. CaM, calmodulin; CCE, capacitative Ca^{2+} entry; SGC, soluble guanylyl cyclase; GTP, guanosine 5′-triphosphate; IP_3R, inositol 1,4,5-triphosphate receptors; NSCC, non-selective Ca^{2+} channels; $ONOO^-$, peroxynitrite; O_2^- superoxide.

Our results suggest that *t*-Resv did not activate SIRT1, at least in a matter of minutes, and therefore, the $[Ca^{2+}]_c$ rise and NO release induced by *t*-Resv seem to be independent of SIRT1. In fact, *t*-Resv-dependent SIRT1 effects described in the literature are generally observed after long-term treatments (i.e. more than 24 h), since effects derived from the deacetylation of histones and transcription factors occur over hours [44, 45].

The inability of *t*-Resv to activate recombinant bovine eNOS in vitro suggests that its NO generating effect is not mediated by a direct, acute stimulation of enzyme activity. In good agreement with this conclusion is the observation that *t*-Resv does not modify rat aorta eNOS activity [8].

The *t*-Resv-induced simultaneous increase in $[Ca^{2+}]_c$ and NO biosynthesis and release could be important in its endothelium-dependent vasorelaxant properties. Substances that increase endothelial cell $[Ca^{2+}]_c$ affect underlying vascular tone, as reported for the ionophore A23187 and for thapsigargin, which induce endothelium-dependent relaxation of guinea-pig rat aorta [46, 47]. Within support of our results, it has been reported that the ability of *t*-Resv to relax rat aorta, porcine coronary artery, porcine retinal arterioles, human internal mammary artery, mesenteric and uterine guinea-pig arteries and saphenous vein rings is partially endothelium-dependent and mediated by a release of NO [6, 8, 11–14, 48] (also, see Introduction). Furthermore, *t*-Resv enhanced agonist-stimulated $[Ca^{2+}]_c$ increases that might trigger NO biosynthesis in rat heart valve endothelial cells [49].

The increase in endothelial $[Ca^{2+}]_c$ induced by *t*-Resv could be also responsible, at least in part, for the red wine polyphenol-induced increase of $[Ca^{2+}]_c$ and the subsequent release of NO and endothelial relaxant factors in bovine aortic endothelial cells [50, 51].

The effects of *t*-Resv on Ca^{2+} handling and NO release in endothelial cells are schematised in Fig. 7, which briefly summarises the findings presented in this study as well as previous work [6, 8, 10, 16, 23, 24].

We have demonstrated, for the first time, that *t*-Resv induces a concentration-dependent, simultaneous increase in $[Ca^{2+}]_c$ and NO release in HUVECs. This effect is mainly mediated by the release of Ca^{2+} from thapsigargin-sensitive intracellular stores and the subsequent activation of store-operated Ca^{2+} entry, although the activation of other plasma membrane Ca^{2+}-permeable channels cannot be ruled out. We have also shown that the activation of AMPK and ERK1/2 also participates in the *t*-Resv increase in NO production. The overall effects of *t*-Resv described here may explain, in part, its endothelium-dependent vasorelaxant effects in isolated rat aortic rings. Bearing in mind that *t*-Resv has been reported to have beneficial effects in the cardiovascular system through a NO-dependent mechanism [52, 53], and assuming that *t*-Resv exhibits similar behaviour in humans in vivo, we suggest that the endothelial NO release described here may be partially involved in these effects. However, it is important to note that the effects described in this study were obtained with concentrations of *t*-Resv considerably higher than those measured in human plasma after normal dietary intake [54, 55]. This suggests that the potential beneficial effect of resveratrol on the vascular endothelium will not be achieved after its dietary consumption, such as a moderate wine intake, and that a pharmacological intervention could be necessary to reach higher plasma levels. It can be also concluded that *t*-Resv may have interesting potential as an original chemical model for the design and subsequent development of new drugs with beneficial cardiovascular properties.

This work was supported by grants from the Ministerio de Ciencia e Innovación, Spain (SAF2010-22051) and Xunta de Galicia, Spain (INCITE08PXIB203092PR and 08CSA019203PR). J. E. and V. G. M. were supported by an FPU pre-doctoral scholarship from the Ministerio de Educación, Spain.

The authors have declared no conflict of interest.

5 References

[1] Siemann, E. H., Creasy, L. L., Concentration of the phytoalexin resveratrol in wine. *Am. J. Enol. Vitic.* 1992, *43*, 49–52.

[2] Soleas, G. J., Diamandis, E. P., Goldberg, D. M., Wine as a biological fluid: history, production, and role in disease prevention. *J. Clin. Lab. Anal.* 1997, *11*, 287–313.

[3] Ibern-Gómez, M., Roig-Pérez, S., Lamuela-Raventós, R. M., de la Torre-Boronat, M. C., Resveratrol and piceid levels in natural and blended peanut butters. *J. Agric. Food Chem.* 2000, *48*, 6352–6354.

[4] Soleas, G. J., Diamandis, E. P., Goldberg, D. M., The world of resveratrol. *Adv. Exp. Med. Biol.* 2001, *492*, 159–182.

[5] Bertelli, A. A., Das, D. K., Grapes, wines, resveratrol and heart health. *J. Cardiovasc. Pharmacol* 2009, *54*, 468–476.

[6] Campos-Toimil, M., Elíes, J., Orallo, F., in: Singh, V. K., Govil, J. N. (Eds.), *Cardiovascular Effects of trans- and cis-Resveratrol. Phytopharmacology and Therapeutic Values III, Vol. 21*, Studium Press LLC, Houston, TX, USA 2008, pp. 263–294.

[7] Delmas, D., Jannin, B., Latruffe, N., Resveratrol: preventing properties against vascular alterations and ageing. *Mol. Nutr. Food Res.* 2005, *49*, 377–395.

[8] Orallo, F., Álvarez, E., Camiña, M., Leiro, J. M. et al., The possible implication of *trans*-resveratrol in the cardioprotective effects of long-term moderate wine consumption. *Mol. Pharmacol.* 2002, *61*, 294–302.

[9] Chen, C. K., Pace-Asciak, C. R., Vasorelaxing activity of resveratrol and quercetin in isolated rat aorta. *Gen. Pharmacol.* 1996, *27*, 363–366.

[10] Orallo, F., Camiña, M., Study of the endothelium-dependent and endothelium-independent vasodilator effects of resveratrol in rat aorta. *Br. J. Pharmacol.* 1998, *124*, 108P.

[11] Li, H. F., Tian, Z. F., Qiu, X. Q., Wu, J. X. et al., A study of mechanisms involved in vasodilatation induced by resveratrol in isolated porcine coronary artery. *Physiol. Res.* 2006, *55*, 365–372.

[12] Naderali, E. K., Smith, S. L., Doyle, P. J., Williams, G., The mechanism of resveratrol-induced vasorelaxation differs in the mesenteric resistance arteries of lean and obese rats. *Clin. Sci. (Lond.)* 2001, *100*, 55–60.

[13] Nagaoka, T., Hein, T. W., Yoshida, A., Kuo, L., Resveratrol, a component of red wine, elicits dilation of isolated porcine retinal arterioles: role of nitric oxide and potassium channels. *Invest. Ophthalmol. Vis. Sci.* 2007, *48*, 4232–4239.

[14] Rakici, O., Kiziltepe, U., Coskun, B., Aslamaci, S. et al., Effects of resveratrol on vascular tone and endothelial function of human saphenous vein and internal mammary artery. *Int. J. Cardiol.* 2005, *105*, 209–215.

[15] Leblais, V., Krisa, S., Valls, J., Courtois, A. et al., Relaxation induced by red wine polyphenolic compounds in rat pulmonary arteries: lack of inhibition by NO-synthase inhibitor. *Fundam. Clin. Pharmacol.* 2008, *22*, 25–35.

[16] Orallo, F., Comparative studies of the antioxidant effects of *cis*- and *trans*-resveratrol. *Curr. Med. Chem.* 2006, *13*, 87–98.

[17] Schmitt, C. A., Heiss, E. H., Dirsch, V. M., Effect of resveratrol on endothelial cell function: molecular mechanisms. *Biofactors* 2010, *36*, 342–349.

[18] Klinge, C. M., Wickramasinghe, N. S., Ivanova, M. M., Dougherty, S. M., Resveratrol stimulates nitric oxide production by increasing estrogen receptor alpha-Src-caveolin-1 interaction and phosphorylation in human umbilical vein endothelial cells. *FASEB J.* 2008, *22*, 2185–2197.

[19] Xu, Q., Hao, X., Yang, Q., Si, L., Resveratrol prevents hyperglycemia-induced endothelial dysfunction via activation of adenosine monophosphate-activated protein kinase. *Biochem. Biophys. Res. Commun.* 2009, *388*, 389–394.

[20] Borra, M. T., Smith, B. C., Denu, J. M., Mechanism of human SIRT1 activation by resveratrol. *J. Biol. Chem.* 2005, *280*, 17187–17195.

[21] Liu, Z., Zhang, L. P., Ma, H. J., Wang, C. et al., Resveratrol reduces intracellular free calcium concentration in rat ventricular myocytes. *Sheng Li Xue. Bao.* 2005, *57*, 599–604.

[22] Zhang, L. P., Yin, J. X., Liu, Z., Zhang, Y. et al., Effect of resveratrol on L-type calcium current in rat ventricular myocytes. *Acta Pharmacol. Sin.* 2006, *27*, 179–183.

[23] Campos-Toimil, M., Elíes, J., Álvarez, E., Verde, I. et al., Effects of *trans*- and *cis*-resveratrol on Ca^{2+} handling in A7r5 vascular myocytes. *Eur. J. Pharmacol.* 2007, *577*, 91–99.

[24] Campos-Toimil, M., Elíes, J., Orallo, F., *Trans*- and *cis*-resveratrol increase cytoplasmic calcium levels in A7r5 vascular smooth muscle cells. *Mol. Nutr. Food Res.* 2005, *49*, 396–404.

[25] Fleming, I., Busse, R., Molecular mechanisms involved in the regulation of the endothelial nitric oxide synthase. *Am. J. Physiol. Regul. Integr. Comp. Physiol.* 2003, *284*, R1–R12.

[26] Kolluru, G. K., Siamwala, J. H., Chatterjee, S., eNOS phosphorylation in health and disease. *Biochimie* 2010, *92*, 1186–1198.

[27] Gifford, S. M., Grummer, M. A., Pierre, S. A., Austin, J. L. et al., Functional characterization of HUVEC-CS: Ca^{2+} signaling, ERK 1/2 activation, mitogenesis and vasodilator production. *J. Endocrinol.* 2004, *182*, 485–499.

[28] Grynkiewicz, G., Poenie, M., Tsien, R. Y., A new generation of Ca^{2+} indicators with greatly improved fluorescence properties. *J. Biol. Chem.* 1985, *260*, 3440–3450.

[29] Kojima, H., Nakatsubo, N., Kikuchi, K., Kawahara, S. et al., Detection and imaging of nitric oxide with novel fluorescent indicators: diaminofluoresceins. *Anal. Chem.* 1998, *70*, 2446–2453.

[30] Räthel, T. R., Leikert, J. J., Vollmar, A. M., Dirsch, V. M., Application of 4,5-diaminofluorescein to reliably measure nitric oxide released from endothelial cells in vitro. *Biol. Proced. Online* 2003, *5*, 136–142.

[31] Putney, J. W., Capacitative calcium entry: from concept to molecules. *Immunol. Rev.* 2009, *231*, 10–22.

[32] Arakaki, N., Nagao, T., Niki, R., Toyofuku, A. et al., Possible role of cell surface H^+-ATP synthase in the extracellular ATP synthesis and proliferation of human umbilical vein endothelial cells. *Mol. Cancer Res.* 2003, *1*, 931–939.

[33] Zini, R., Morin, C., Bertelli, A., Bertelli, A. A. et al., Effects of resveratrol on the rat brain respiratory chain. *Drugs Exp. Clin. Res.* 1999, *25*, 87–97.

[34] Chiou, C. Y., Malagodi, M. H., Studies on the mechanism of action of a new Ca^{2+} antagonist, 8-(*N*,*N*-diethylamino)-octyl 3,4,5-trimethoxybenzoate hydrochloride in smooth and skeletal muscles. *Br. J. Pharmacol.* 1975, *53*, 279–285.

[35] Low, A. M., Berdik, M., Sormaz, L., Gataiance, S. et al., Plant alkaloids, tetrandrine and hernandezine, inhibit calcium-depletion stimulated calcium entry in human and bovine endothelial cells. *Life Sci.* 1996, *58*, 2327–2335.

[36] Lin, S., Fagan, K. A., Li, K. X., Shaul, P. W. et al., Sustained endothelial nitric-oxide synthase activation requires capacitative Ca^{2+} entry. *J. Biol. Chem.* 2000, *275*, 17979–17985.

[37] Tiruppathi, C., Ahmmed,G. U., Vogel, S. M., Malik, A. B., Ca^{2+} signaling, TRP channels, and endothelial permeability. *Microcirculation* 2006, *13*, 693–708.

[38] Dreher, D., Junod, A. F., Differential effects of superoxide, hydrogen peroxide, and hydroxyl radical on intracellular calcium in human endothelial cells. *J. Cell Physiol.* 1995, *162*, 147–153.

[39] Graier, W. F., Hoebel, B. G., Paltauf-Doburzynska, J., Kostner, G. M., Effects of superoxide anions on endothelial Ca^{2+} signaling pathways. *Arterioscler. Thromb. Vasc. Biol.* 1998, *18*, 1470–1479.

[40] Wallerath, T., Deckert, G., Ternes, T., Anderson, H. et al., Resveratrol, a polyphenolic phytoalexin present in red

wine, enhances expression and activity of endothelial nitric oxide synthase. *Circulation* 2002, *106*, 1652–1658.

[41] Leikert, J. F., Rathel, T. R., Wohlfart, P., Cheynier, V. et al., Red wine polyphenols enhance endothelial nitric oxide synthase expression and subsequent nitric oxide release from endothelial cells. *Circulation* 2002, *106*, 1614–1617.

[42] Wallerath, T., Li, H., Godtel-Ambrust, U., Schwarz, P. M. et al., A blend of polyphenolic compounds explains the stimulatory effect of red wine on human endothelial NO synthase. *Nitric Oxide* 2005, *12*, 97–104.

[43] Zou, J. G., Wang, Z. R., Huang, Y. Z., Cao, K. J. et al., Effect of red wine and wine polyphenol resveratrol on endothelial function in hypercholesterolemic rabbits. *Int. J. Mol. Med.* 2003, *11*, 317–320.

[44] Chung, S., Yao, H., Caito, S., Hwang, J. W. et al., Regulation of SIRT1 in cellular functions: role of polyphenols. *Arch. Biochem. Biophys.* 2010, *501*, 79–90.

[45] Mannari, C., Bertelli, A. A., Stiaccini, G., Giovannini, L., Wine, sirtuins and nephroprotection: not only resveratrol. *Med. Hypotheses* 2010, *75*, 636–638.

[46] Taniguchi, H., Hirano, H., Tanaka, Y., Tanaka, H. et al., Possible involvement of Ca^{2+} entry and its pharmacological characteristics responsible for endothelium-dependent, NO-mediated relaxation induced by thapsigargin in guinea-pig aorta. *J. Pharm. Pharmacol.* 1999, *51*, 831–840.

[47] Taniguchi, H., Tanaka, Y., Hirano, H., Tanaka, H. et al., Evidence for a contribution of store-operated Ca^{2+} channels to NO-mediated endothelium-dependent relaxation of guinea-pig aorta in response to a Ca^{2+} ionophore, A23187. *Naunyn-Schmiedebergs Arch. Pharmacol.* 1999, *360*, 69–79.

[48] Naderali, E. K., Doyle, P. J., Williams, G., Resveratrol induces vasorelaxation of mesenteric and uterine arteries from female guinea-pigs. *Clin. Sci. (Lond.)* 2000, *98*, 537–543.

[49] Buluc, M., Demirel-Yilmaz, E., Resveratrol decreases calcium sensitivity of vascular smooth muscle and enhances cytosolic calcium increase in endothelium. *Vascul. Pharmacol.* 2006, *44*, 231–237.

[50] Duarte, J., Andriambeloson, E., Diebolt, M., Andriantsitohaina, R., Wine polyphenols stimulate superoxide anion production to promote calcium signaling and endothelial-dependent vasodilatation. *Physiol. Res.* 2004, *53*, 595–602.

[51] Martin, S., Andriambeloson, E., Takeda, K., Andriantsitohaina, R., Red wine polyphenols increase calcium in bovine aortic endothelial cells: a basis to elucidate signalling pathways leading to nitric oxide production. *Br. J. Pharmacol.* 2002, *135*, 1579–1587.

[52] Das, D. K., Maulik, N., Resveratrol in cardioprotection: a therapeutic promise of alternative medicine. *Mol. Interv.* 2006, *6*, 36–47.

[53] Wang, S., Wang, X., Yan, J., Xie, X. et al., Resveratrol inhibits proliferation of cultured rat cardiac fibroblasts: correlated with NO-cGMP signaling pathway. *Eur. J. Pharmacol.* 2007, *567*, 26–35.

[54] Fernández-Morales, J. C., Yánez, M., Orallo, F., Cortès, L. et al., Blockade by nanomolar resveratrol of quantal catecholamine release in chromaffin cells. *Mol. Pharmacol.* 2010, *78*, 734–744.

[55] Wong, R. H., Howe, P. R., Buckley, J. D., Coates, A. M. et al., Acute resveratrol supplementation improves flow-mediated dilatation in overweight/obese individuals with mildly elevated blood pressure. *Nutr. Metab. Cardiovasc. Dis.* 2011, in press, DOI: 10.1016/j.numecd.2010.03.003.

